Energy harvesting in silicon wavelength converters

Kevin K. Tsia, Sasan Fathpour, and Bahram Jalali

Optoelectronic Circuits and Systems Laboratory
Electrical Engineering Department
University of California, Los Angeles, CA, 90095 USA
tsia@ee.ucla.edu, sasan@ee.ucla.edu, jalali@ucla.edu

http://www.ee.ucla.edu/~oecs/

Abstract: Nonlinear loss is the central problem in silicon devices that operate using nonlinear optical effects. Wavelength converters are one example of such devices, wherein high optical intensities required for nonlinear interactions cause two-photon absorption and severe free-carrier absorption. In this paper, we report the first demonstration of nonlinear photovoltaic effect in silicon wavelength converters. This useful phenomenon allows us to eliminate the nonlinear loss caused by free-carrier absorption, while harvesting the optical power that is normally consumed by two-photon absorption.

OCIS codes: (130.4310) Integrated optics, nonlinear; (190.4380) Nonlinear optics, four-wave mixing; (230.4320) Nonlinear optical devices; (190.2620) Frequency conversion

References and links

1. L. Pavesi and G. Guillot, *Optical interconnects: the Silicon approach* (Springer, 2006).
2. G. T. Reed and A. P. Knights, *Silicon Photonics: An Introduction*, Chichester, U.K. (Wiley 2004).
3. R. L. Espinola, J. I. Dadap, R. M. Osgood, Jr., S. J. McNab, and Y. A. Vlasov, "C-band wavelength conversion in silicon photonic wire waveguides," Opt. Express **13**, 4341-4349 (2005). http://www.opticsinfobase.org/abstract.cfm?URI=oe-13-11-4341
4. K. Yamada, H. Fukuda, T. Tsuchizawa, T. Watanabe, T. Shoji, and S. Itabashi, "All-optical efficient wavelength conversion using silicon photonic wire waveguide," IEEE Photon. Technol. Lett., **18**, 1046-1048, (2006).
5. H. Rong, Y. -H. Kuo, A. Liu, M. Paniccia, and O. Cohen, "High efficiency wavelength conversion of 10 Gb/s data in silicon waveguides," Opt. Express **14**, 1182-1188 (2006). http://www.opticsinfobase.org/abstract.cfm?URI=oe-14-3-1182
6. M. A. Foster, A. C. Turner, J. E. Sharping, B. S. Schmidt, M. Lipson , A. L. Gaeta, "Broad-band optical parametric gain on a silicon photonic chip," Nature, **441**, 960-963 (2006).
7. T. K. Liang, H. K. Tsang, "Role of free carriers from two-photon absorption in Raman amplification in silicon-on-insulator waveguides," Appl. Phys. Lett. **84**, 2745-2747 (2004).
8. R. Claps, V. Raghunathan, D. Dimitropoulos, and B. Jalali, "Influence of nonlinear absorption on Raman amplification in Silicon waveguides," Opt. Express **12**, 2774-2780 (2004). http://www.opticsinfobase.org/abstract.cfm?URI=oe-12-12-2774
9. R. Jones, H. Rong, A. Liu, A. Fang, M. Paniccia, D. Hak, and O. Cohen, "Net continuous wave optical gain in a low loss silicon-on-insulator waveguide by stimulated Raman scattering," Opt. Express **13**, 519-525 (2005). http://www.opticsinfobase.org/abstract.cfm?URI=oe-13-2-519
10. H. Rong, R. Jones, A. Liu, O. Cohen, D. Hak, A. Fang and M. Paniccia, "A continuous-wave Raman silicon laser," Nature **433**, 725-728 (2005).
11. S. Fathpour, O. Boyraz, D. Dimitropoulos, and B. Jalali, "Demonstration of CW Raman gain with zero electrical power dissipation in p-i-n silicon waveguides," in *Proceedings of IEEE Conf. on Lasers and Electro-optics, CLEO 2006*, Long Beach, CA, May 2006, paper CMK3.
12. International Technology Roadmap for Semiconductors, 2005 Edition, http://www.itrs.net/.
13. D. J. Frank, "Scaling CMOS to the Limits," *IBM J. Research and Development* **46**, 235-244 (2002).
14. S. Fathpour, K. K. Tsia, and B. Jalali, *presented at Optical Amplifiers and Their Applications Topical Meeting (OAA)*, Whistler, B.C., Canada, June 2006, paper PD1**.**
15. S. Fathpour, K. K. Tsia, and B. Jalali, "Energy harvesting in silicon Raman amplifiers", Appl. Phys. Lett. **89**, 061109 (2006).
16. G. P. Agrawal, *Nonlinear Fiber Optics*, 3rd edition (Academic Press, New York, 2001).
17. R. Claps, V. Raghunathan, O. Boyraz, P. Koonath, D. Dimitropoulos, and B. Jalali, "Raman amplification and lasing in SiGe waveguides," Opt. Express, **13**. 2459–2466 (2005). http://www.opticsinfobase.org/abstract.cfm?URI=oe-13-7-2459

#75263 - $15.00 USD Received 21 September 2006; revised 28 October 2006; accepted 7 November 2006

18. Q. Lin, J. Zhang, P. M. Fauchet, and G. P. Agrawal, "Ultrabroadband parametric generation and wavelength conversion in silicon waveguides," Opt. Express **14**, 4786-4799 (2006). http://www.opticsinfobase.org/abstract.cfm?URI=oe-14-11-4786
19. D. Dimitropoulos, S. Fathpour, and B. Jalali, "Limitations of active removal in silicon Raman amplifiers and lasers," Appl. Phys. Lett. **87**, 261108 (2005).
20. M. Dinu, F. Quochi, and H. Garcia, "Third-order nonlinearities in silicon at telecom wavelengths," Appl. Phys. Lett., **82**, 2954-2956 (2003).
21. D. Dimitropoulos, V. Raghunathan, R. Claps, and B. Jalali, "Phase-matching and Nonlinear Optical Processes in Silicon Waveguides," Opt. Express **12**, 149-160 (2004). http://www.opticsinfobase.org/abstract.cfm?URI=oe-12-1-149
22. J. Hansryd, P. A. Andrekson, M. Westlund, J. Li, and P- O. Hedekvist, "Fiber-based optical parametric amplifiers and their applications," IEEE J. Sel. Top. Quantum Electron., **8**, 506-520 (2002).

1. Introduction

The past five years have witnessed an explosion of progress in all aspects of silicon photonics, including photodetectors and modulators as well as a new class of active devices that exploit the strong third-order optical nonlinearities of silicon [1,2]. These include Raman-based optical amplifiers and lasers [1,2] as well as wavelength converters based on the Kerr effect [3-6]. A common feature of all these devices is the high optical intensities inside the waveguide leading to two highly undesirable effects. The first is the loss of photons due to two-photon absorption (TPA). The second is a more severe optical absorption caused by the free carriers that are generated by TPA. Free-carrier absorption (FCA) is a particularly detrimental effect in silicon Raman amplifiers and lasers, and normally prevents continuous-wave (CW) amplification and lasing. In order to reduce FCA, sweep-out of the induced free carriers by a reverse biased *p-n* junction has been proposed [7,8] and demonstrated [9-11]. It has also been shown that carrier sweep-out results in modest improvement in the efficiency of wavelength conversion achieved via four-wave mixing (FWM) [5].

However, little or no attention has been made to the power dissipation of nonlinear silicon-photonic devices. For instance, in reference [10], about one Watt of electrical power had to be dissipated (25V at ~40 mA) to achieve ~4 dB of CW optical gain and produce ~ 8 mW of output from a Raman laser. Such high power dissipations are incompatible with the power dissipation constraints currently faced by the very silicon chips. The problem of chip heating is so severe that it threatens to stop future advances in the technology as described the by the celebrated Moore's law [12]. The fact is highlighted by the recent shift of the microprocessor industry away from increasing the clock speed and in favor of multi-core processors [13]. To be sure, realization of low-power silicon photonic devices is of paramount importance if opto-electronic integration is to take place.

Here, we address this problem in the context of silicon wavelength converters. We describe a new phenomenon in silicon wavelength converter that makes it possible to not only mitigate the TPA problem, but paradoxically, to take advantage of it. We show that it is possible to realize a nonlinear photovoltaic effect arising from TPA in waveguide *p-n* junction devices. Through this effect, electrical power can be harvested from the device. Power generation occurs not at the expense of carrier sweep-out, but rather because of it. Recently, we showed that such phenomenon occurs in silicon Raman devices [14-15]. The present work shows that energy harvesting can also be achieved in Kerr-based devices such as wavelength converters.

To recover the energy that is lost to TPA, the present device converts the absorbed optical power into useable electrical power, in much the same manner as a solar cell. However, it should be clear that the purpose here is not to propose a new solar cell, but rather to describe a method for realizing energy efficient wavelength converters in silicon.

#75263 - $15.00 USD Received 21 September 2006; revised 28 October 2006; accepted 7 November 2006

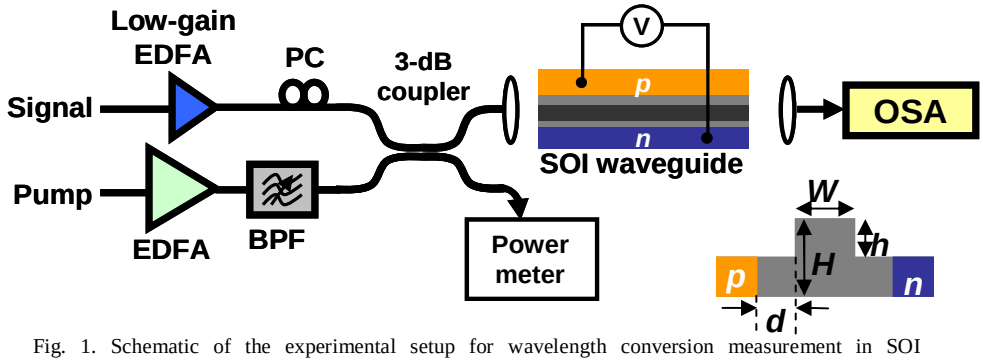

Fig. 1. Schematic of the experimental setup for wavelength conversion measurement in SOI waveguides (EDFA: Erbium-doped fiber amplifier; BPF: band pass filter; PC: polarization controller; OSA: optical spectrum analyzer). The right bottom inset shows the rib waveguide cross-section with width of W = 1.5 μm, rib height of H = 2 μm, etch-depth of h = 0.9μm and d = 1.9 μm.

2. Experiments and results

Wavelength conversion via FWM was measured in straight rib waveguides, with a lateral *p-i-n* junction diode, as shown in Fig. 1. The devices were fabricated on a SOI wafer by standard photolithography, dry etching, dopant implantation, passivation and metallization techniques. The *p-i-n* diode is formed by heavily-doped n^+- and p^+-region defined on each side of the rib, respectively, with a distance d from the rib edge. Different variation of waveguide width W = 1.5 μm – 3.0 μm and d = 1.6 μm – 2.8 μm were obtained. Laterally-tapered mode-converters were used in order to reduce coupling losses into and out of the waveguides. The facets were polished but were left uncoated. The experimental results presented in the following are for 3-cm long waveguides with width of W = 1.5 μm, rib height of H = 2 μm, etch-depth of h = 0.9 μm and d = 1.9 μm. The linear propagation loss of the waveguide was measured to be 0.5 dB/cm based on Fabry-Pérot resonance technique.

The experimental setup is depicted in Fig. 1. A distributed feedback (DFB) fiber laser at 1545.29 nm is amplified by an Erbium-doped fiber amplifier (EDFA) to produce a pump beam with power up to 5 W. The signal beam is generated from an external cavity tunable diode laser, with a tuning range about 100 nm, followed by a low-gain EDFA. The pump and signal beams are combined by a 3-dB coupler followed by two identical objective lenses (NA = 0.40) to couple the light into and out of the

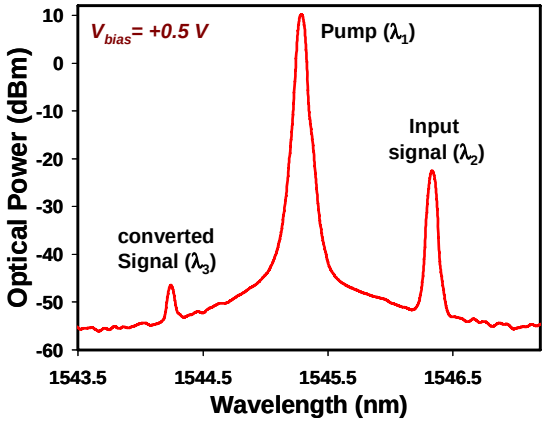

Fig. 2. Output spectrum resulted from four-wave mixing in the waveguide under forward-bias of V_{bias} = + 0.5V at coupled pump power of 0.71W. The converted signal is at 1544.25 nm with a conversion efficiency ~ –23.8dB.

#75263 - $15.00 USD Received 21 September 2006; revised 28 October 2006; accepted 7 November 2006

waveguides. The output spectrum is analyzed by an optical spectrum analyzer (OSA). The input pump power is monitored by a power meter at another output port of the 3-dB coupler. The polarization of the signal beam is aligned to the TE waveguide mode. The electrical loop that biases the *p-i-n* diodes consists of a power supply, a current meter and a 100 Ω series resistor. The photovoltaic effect is realized by operating the *p-i-n* diode in the fourth quadrant of its current-voltage (*I-V*) characteristics, where the diode is forward biased but below its turn-on voltage of ~0.7 V. The key concept is that although the diode is forward biased, the TPA generated carriers are swept out because its internal current is in the reverse direction.

Figure 2 shows a typical FWM output spectrum measured under a forward bias of +0.5 V. A new peak is observed at λ_3 = 1544.25 nm which is consistent with the FWM relation among the pump (λ_1 = 1545.29 nm), the input signal (λ_2 = 1546.34 nm) and the converted signal (idler) wavelength (λ_3), i.e., $1/\lambda_3 = 2/\lambda_1 - 1/\lambda_2$ [16]. The wavelength conversion efficiency, defined as the ratio between the peak of the converted signal at λ_3 and the input signal at λ_2, was measured to be –23.8 dB at a coupled pump power of 0.71W.

Figure 3(a) shows the relationship between the conversion efficiency and the coupled pump power at different biasing conditions. The wavelength detuning between the signal and the pump, $\Delta\lambda$ is 1 nm. The conversion efficiency does not largely depend on the biasing conditions at low coupled pump power regime (< 0.3 W). As expected, the loss introduced by the TPA-generated free carriers at open-circuit results in the saturation of the conversion efficiency at ~ –25 dB for high pump powers. At a reverse bias of –15 V, efficient carrier sweep-out leads to a conversion efficiency of –21.4 dB (at 0.71 W coupled pump power) without substantial saturation. The slope of the efficiency plot at this bias is ~1.91, which is close to the ideal quadratic relation of the efficiency versus pump power in FWM process [16]. Figure 3(b) shows the conversion spectra at different biasing conditions. The detuning characteristics qualitatively agree with the $sinc^2$ function behavior predicted theoretically [16]. The 3-dB bandwidth is about 11 nm and is insensitive to the biasing conditions.

Conversion efficiency has a strong dependence on carrier lifetime. The lifetime values were measured from pump-probe experiments conducted on the same waveguides at different biases. The details of the technique can be found elsewhere [17]. Figure 4 depicts the change in a CW probe beam caused by a pump pulse. The responses consist of a fast transient dip caused by TPA, and a slow recovery associated with the recombination of TPA generated carriers. Carrier lifetime values

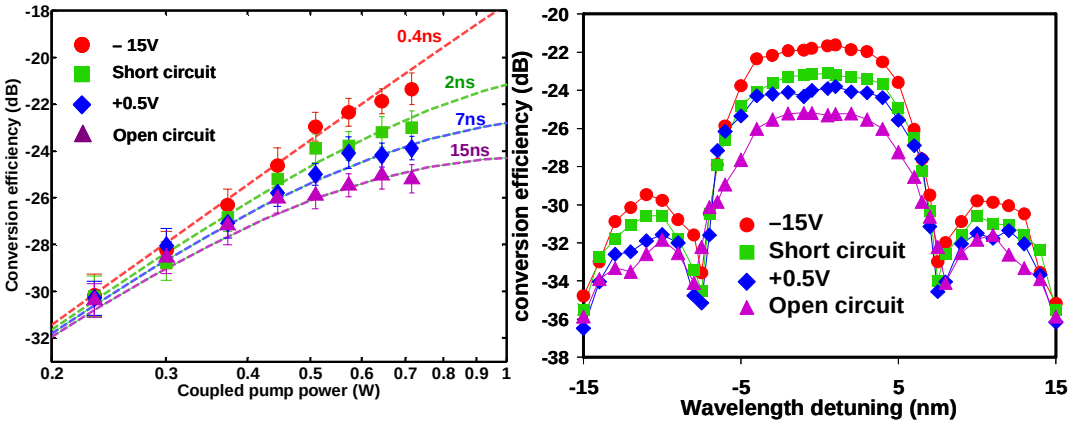

(a) (b)

Fig. 3. Wavelength conversion efficiency as a function of coupled pump power under different biasing conditions. The wavelength detuning, $\Delta\lambda=\lambda_2-\lambda_1$, is 1 nm. The dashed lines represent the modeled conversion efficiency for different measured carrier lifetime values at different biasing conditions. (b) Wavelength conversion efficiency as a function of the wavelength detuning $\Delta\lambda$ at different biasing conditions, measured at pump power of 0.71 W.

#75263 - $15.00 USD Received 21 September 2006; revised 28 October 2006; accepted 7 November 2006

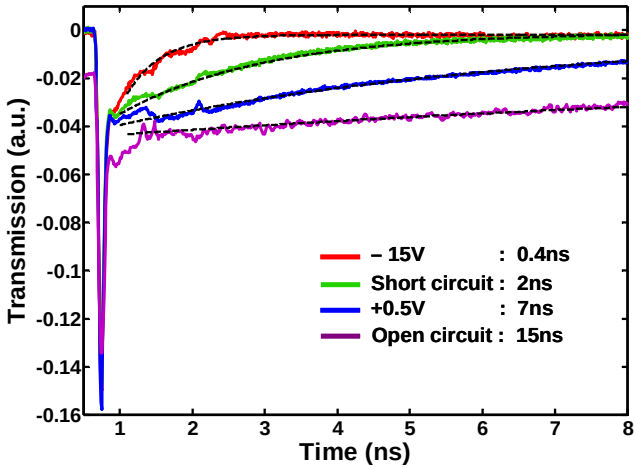

Fig. 4. Temporal response of a CW signal laser to a pulsed pump laser at different biasing condition in the *p-i-n* SOI waveguide. The fitted carrier lifetime values are shown in the legend.

were extracted by fitting the slow recovery part of the curve and were fed into the theoretical model. As described in Section 3 (below), the conversion efficiency predicted by the model is in good agreement with the experimental observations.

Referring to Fig. 4, we find that the lifetime at +0.5 V is about 7 ns, while it is 15 ns under open circuit condition. Shorter lifetime gives rise to a lower free carrier density and hence lower FCA. It results in ~ 1.3-1.5 dB improvement in the conversion efficiency under a forward bias of +0.5 V at high pump powers, as compared with the open-circuit case (Fig. 3(a)). The improvement in efficiency under forward bias should not be surprising since the prerequisite for carrier sweep-out is negative diode photocurrent and not negative voltage [14-15]. As long as the forward voltage is below the turn-on voltage (~0.7 V), free carriers are partially swept out leading to a reduction in carrier density. The measured *I-V* characteristics of the diode in the presence of the pump (Fig. 5(a)), clearly shows that a *reverse* current does flow through the device despite of the applied *forward* voltage. This is clear evidence that these devices posses a nonlinear photovoltaic effect that is caused by the sweep-out of the TPA-generated carriers by the built-in electric field of the *p-n* junction. The

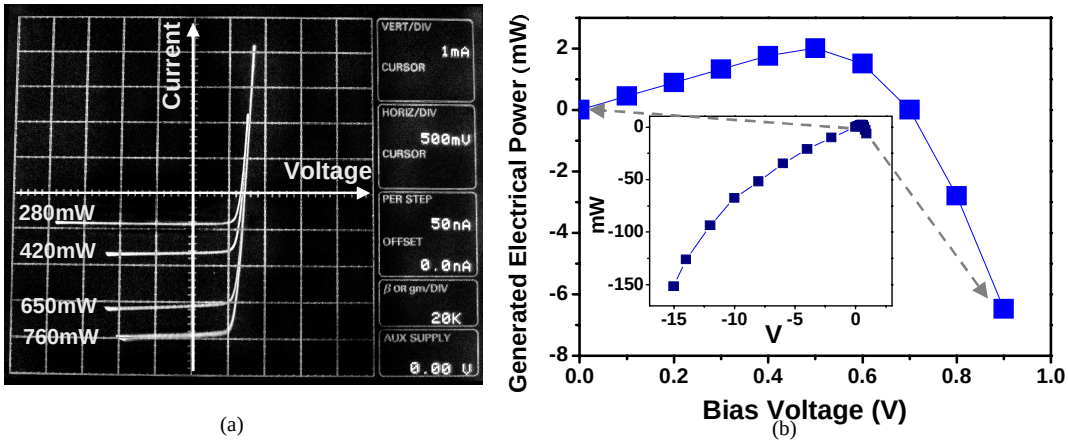

(a) (b)

Fig. 5. (a) *I-V* characteristics of the *p-i-n* diode straddled the SOI rib waveguide at various coupled pump powers measured by a curve-tracer. (b) Generated electrical power from the diode as a function of forward bias at $\Delta\lambda$ =1 nm and coupled pump power of 0.71W. The inset shows the generated electrical power in wider range of bias voltages, from –15V to + 0.9 V.

#75263 - $15.00 USD Received 21 September 2006; revised 28 October 2006; accepted 7 November 2006

observation is significant because the sweep-out of free carriers by the built-in field results in generation of electrical power. In contrast, when the sweep-out is achieved with an applied reverse voltage, then electrical power is consumed. As shown in Fig. 5(b), while ~160 mW of power is dissipated under reverse voltage of –15 V (inset), an electrical power of 2 mW is generated at +0.5 V, harvested from the photons that were lost to TPA. These findings have obvious impact in creating low power silicon photonic devices.

3. Analysis and discussion

The evolution of the pump A_p, signal A_s and idler A_i fields along the waveguide can be described by the coupled-mode equations [16, 18]:

$$\frac{dA_p}{dz} = -\frac{1}{2}\left[\alpha + \alpha_p^{FCA}(z)\right]A_p + i\left(\gamma_p + i\frac{\beta}{2}\right)\left|A_p\right|^2 A_p, \tag{1}$$

$$\frac{dA_s}{dz} = -\frac{1}{2}\left[\alpha + \alpha_s^{FCA}(z)\right]A_s + 2i\left(\gamma_s + i\frac{\beta}{2}\right)\left|A_p\right|^2 A_s + i\gamma_s A_p^{\,2} A_i^* \exp(-i\Delta k \cdot z), \tag{2}$$

$$\frac{dA_i^*}{dz} = -\frac{1}{2}\left[\alpha + \alpha_i^{FCA}(z)\right]A_i^* - 2i\left(\gamma_i - i\frac{\beta}{2}\right)\left|A_p\right|^2 A_i^* - i\gamma_i A_p^{*2} A_s \exp(i\Delta k \cdot z), \tag{3}$$

where the field amplitude A_j is the normalized such that $|A_j|^2$ gives the power in Watts (j = p,s,i). It has been assumed that $|A_p| > |A_s| > |A_i|$. The parameter α (cm^{-1}) is the linear loss and $\alpha_j^{FCA}(z) = 1.45 \times 10^{-17} (\lambda_j / 1.55)^2 \Delta N$ [8]. λ_j is the wavelength (μm). ΔN (cm^{-3}) is the carrier density generated by TPA, given by $\Delta N = \tau_{eff} \beta |A_j|^4 / 2 E_j A_{eff}$ [19], where τ_{eff} is the effective carrier lifetime obtained from the pump-probe measurements (Fig. 4). E_j is the photon energy and A_{eff} is the effective modal area. β = 0.7 cm/GW is the TPA coefficient [7], which is assumed to be constant over the telecommunication band. $\gamma_j = n_2 \omega_p / c$ with nonlinear refractive index $n_2 = 4.5 \times 10^{-14}$ cm^2/W [20]. Δk is the phase mismatch among the three fields, defined as $\Delta k = k_s + k_i - 2k_p$, where k_j is the propagation constant at frequency ω_j. Δk is obtained from a full-vectorial simulation tool that uses the beam propagation method (BeamPROP). Using the measured carrier lifetimes, Eqs. (1) – (3) are used to compute the

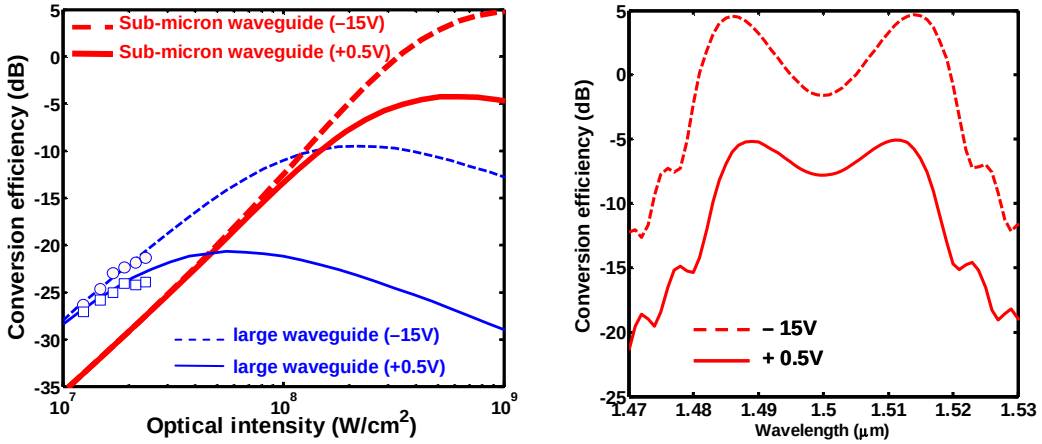

Fig. 6. (a) Conversion efficiency versus optical intensity for a large waveguide (W = 1.5 μm, H = 2 μm, h = 0.9 μm, d = 1.9 μm) and a sub-micron waveguide (W = 0.45 μm, H = 0.35 μm, h = 0.3μm, d = 0.3 μm). The dashed and solid curves represent –15 V and +0.5 V biases, respectively. The experimental data at –15 V (circles) and +0.5V (squares) are overlaid (same as in Fig. 3). $\Delta\lambda$ = 1 nm and 15 nm for large and sub-micron waveguide, respectively; (b) Calculated conversion spectra of the small waveguide at optical intensity of ~300 MW/cm^2 at –15 V (dashed line) and +0.5 V (solid line).

#75263 - $15.00 USD Received 21 September 2006; revised 28 October 2006; accepted 7 November 2006

conversion efficiency versus pump power, the results of which provide insight into the experimental observations described in Fig. 3(a).

The relative low conversion efficiency in the present work, as compared with the recent results [4-6], is somewhat due to the fact that the optical intensity inside our waveguide relatively low (~20 MW/cm^2). This is because of the relatively larger waveguide size and the limitations in the pump source. Calculations show that the efficiency can reach ~ –20 dB at +0.5 V if the optical intensity is increased to ~100 MW/cm^2, beyond which it is limited by FCA (Figure 6(a)).

Further increase in wavelength conversion efficiency requires phase matching. A large normal group velocity dispersion (GVD ~ –800 ps/km-nm at 1.5 μm) of our waveguide, dominated by the material dispersion, results in a low conversion efficiency as well as narrow conversion bandwidth [16, 21]. High wavelength conversion efficiency and bandwidth was recently demonstrated by Gaeta *et al*. through waveguide dispersion engineering [6]. Using the same approach for phase matching, Fig. 6 also shows the conversion efficiency for a sub-micron waveguide (W = 0.45 μm, H = 0.35 μm, h = 0.3μm and d = 0.3μm) that exhibits anomalous GVD (+600 – +900 ps/km-nm from 1.4 – 1.7 μm). We obtain the bias dependent lifetime for this structure by using a drift-diffusion simulator (ATLAS by Silvaco International) [19] and use it in the coupled mode calculations. Figure 6(a) shows that a high conversion efficiency of -5 dB can be achieved at ~300 MW/cm^2 optical intensity and at +0.5V voltage where energy harvesting occurs. At the same time, a wide conversion bandwidth of ~30 nm can also be attained (Fig. 6(b)) under the same conditions. Therefore, high wavelength conversion efficiency, large optical bandwidth, and energy harvesting can be achieved simultaneously.

4. Conclusions

In conclusion, wavelength conversions via four-wave mixing and energy harvesting are simultaneously demonstrated in a silicon device. Pump-induced free carriers are swept out by the built-in field of the junction, thus lower the nonlinear losses at the same time when electrical power is being delivered to an external circuit. The electrical power is harvested from the optical power that is normally lost to TPA. This approach for creating energy efficient silicon photonic devices is applicable to other semiconductor nonlinear photonic devices in which two-photon absorption occurs. A trade-off that exists is that the built-in filed of the diode will be insufficient for carrier sweep-out above certain pump intensity due to screening of the field by the large number of carriers [19].

Acknowledgments

This material is based on research sponsored by DARPA under the EPIC program.

#75263 - $15.00 USD Received 21 September 2006; revised 28 October 2006; accepted 7 November 2006